A Modular Compliant Actuator for Emerging High Performance and Fall-Resilient Humanoids

F.Negrello[1], M.Garabini[2], M.G.Catalano[1], J.Malzahn[1], D.G.Caldwell[1], A.Bicchi[1,2] and N.G.Tsagarakis[1]

***Abstract*— The application of humanoids in real world environments necessarily requires robots that can demonstrate physical resilience against strong physical interactions with the environment and impacts, that may occur during falling incidents, that are unavoidable. This paper introduces a modular high performance actuation unit designed to be robust against impacts and strong physical perturbations. The protection against impacts is achieved with the use of elastic transmission combined with soft cover elements on the link side. The paper introduce the details of the actuator design and implementation and discuss the effects of the soft cover and series elastic transmission on the reduction of the impact forces which reach the reduction drive of the actuator during impacts. The model of prototype joint, including the actuator unit, its elastic transmission and the driving link soft cover, is introduced and simulations were performed to study the effect of the elastic properties of the transmission and the soft cover on the reduction of the impact forces transmitted to the reduction drive. The results from the simulations are confirmed by experimental measurements on the real system under induced experimental impact trials, demonstrating the significant effect of the soft cover in the further reduction of impact forces. The performance of the proposed actuator unit in terms of physical robustness makes it ideal for the development of emerging humanoids robots that will be capable of surviving falls and recovers from them.**

I. Introduction

Today the intervention of human responders after incidents occurred after physical and man-made disasters is the only option for resolving these situations. This is due to the limitation of state-of-the-art humanoids under many aspects: ranging from the mechanical design up to control and high level decision strategies. On the hardware side the main problem is related to the lack of reliability and robustness. State of the art robots have very limited capabilities to sustain overloads due to peak forces in case of unpredictable impacts or falls.

On one side the mechanical strength of the most sensitive components of the actuators, usually gearboxes (harmonic drive or planetary gears) used in most humanoids like [1][2][3][4][5][6] set the limit of the actuator robustness. On the other side the conventional position control requiring rigid link and structures to ensure good tracking of the controller input trajectories, the limited sensing capacity, the delays introduced by the propagation of the impact forces and thus the lack of reaction within the first instance of the impact, make these robots unable to adapt to unstructured environment or to non-anticipated physical interactions that evolves dynamically as a result of accidental collisions and falls.

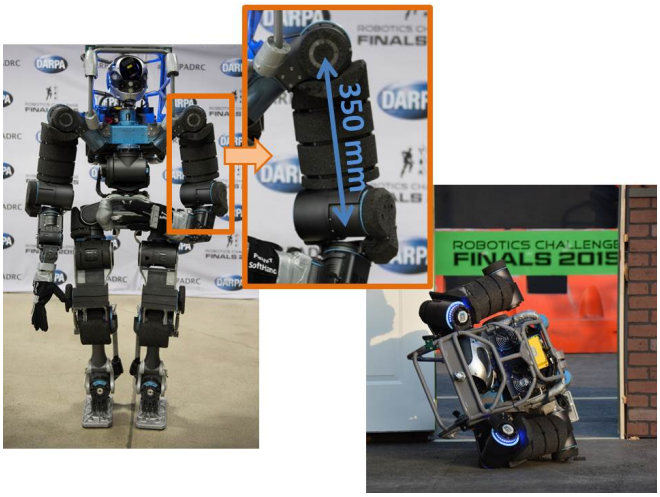

Fig. 1: WALK-MAN the humanoid platform developed at the Italian Institute of Technologies. The robot at the DARPA Robotics Challenge Finals and a falling incident during the execution of the first run.

The robotic community does not underestimate the importance of this challenge. One of the tangible facts that push the research in this direction has been the DARPA Robotics Challenge held in June 2015 [7]. In this competition robots had to sequentially accomplish eight tasks without any kind of protection from falls (gantry systems), except their intrinsic body design. The challenge has shown the necessity to develop multiple and different skills to enhance the autonomy and adaptability of humanoids robot. For instance locomotion skills are required to cope with a variety of terrains and passages with the effective ability to navigate and reach places through stairs and ladders. At the same time manipulation skills are required to cope with tools and interfaces designed for human use. In conclusion physical power, adaptability and robustness against physical interaction are vital requirements as robots in such environment are expected to normally interact with the environments or even accidentally collide or fall and self-recover during these locomotion or manipulation operations, Fig 1.

One of the possible methods to increase the structural

This work is supported by the WALK-MAN FP7-ICT-2013-10 European Commission project.

[1]Department of Advanced Robotics, Istituto Italiano di Tecnologia, Via Morego 30, 16163, Italy, {francesca.negrello, manuel.catalano, Jorn.Malzahn, nikos.tsagarakis, antonio.bicchi, darwin.caldwell}@iit.it

[2]Research Center "Enrico Piaggio", University of Pisa, Largo Lucio Lazzarino 1, 56126 Pisa, Italy, {manolo.garabini, bicchi}@centropiaggio.unipi.it

	A	B	C
Continues Power (W) @ 120C rise	900	500	222
Intermediate Mechanical Power, (G=80:1, eff=70%)	112Nm @ 11.7rad/s 1300W	89Nm @ 11.7rad/s 1040W	30Nm @ 10.2rad/s 305W
Dynamic Peak Mechanical Power, (G=80:1, eff=70%)	220Nm @ 10.4rad/s 2280W	140Nm @ 11.2rad/s 1560W	56Nm @ 8.2rad/s 460W
Peak Torque (Nm), (G=80:1, eff=90%)	270	140	56
No load speed (rpm)	14	16.7	11.3
Weight (kg)	2.0	1.5	0.7
Stiffness (Nm/rad)	2300	1200	500
Overall dimensions DxL (mm)	110x150	100x140	60x100

TABLE I: WALK-MAN Actuation Units: specifications

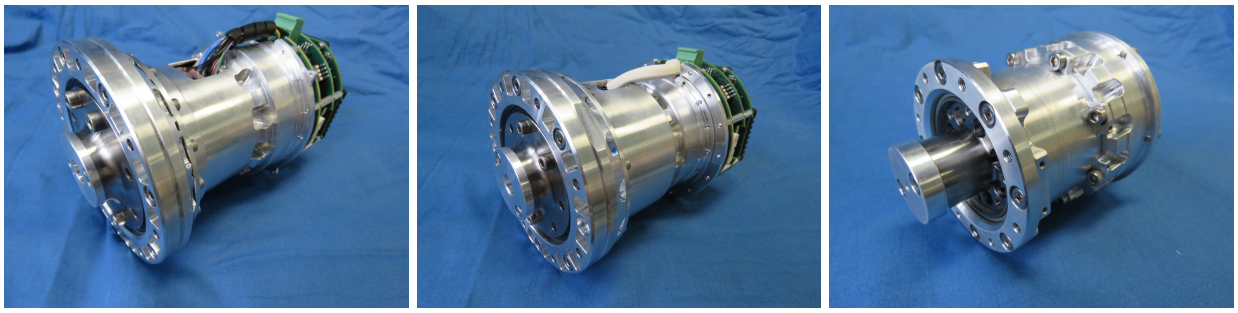

(a) (b) (c)

Fig. 2: WALK-MAN Actuation Units: prototypes

robustness of the robots is to insert compliant elements in their structure or to exploit the intrinsic elasticity of their actuation principle. Series Elastic Actuator (SEA) belongs to this approach, an example is the compliant humanoid COMAN robot [8][9][10]. The leading edge of this technology are the Variable Impedance Actuators (VIA), that allow to tune actively the global impedance of the system on the task specifications [11][12][13][14][15][16]. These actuators still have few applications in full-body humanoids due to the increasing complexity of the system. Recently, new control strategies for humanoids have been developed based on joint torque control to take into account the forces exchanged with the environment during the robot operation [17][18]. Many recent humanoids have therefore embedded in their joints a torque sensor, based on an elastic element sensorized with Strain Gauges, to have direct torque feedback [10][19][20]. Despite the efforts both those methods have disadvantages, the low natural frequency and bandwidth due to the presence of the elasticity in the first case, or the lack of filtering of the first load peak due to a delayed response in the case of the active compliance control based or torque feedback.

The goal of this work is to develop a high power actuation unit, which is capable of producing highly dynamic motions while at the same time being robust against impacts by tuning the mechanical properties of two elastic elements located at the transmission side (SEA) and at the link side (soft cover). To evaluate the effectiveness of these two combined elasticities in the reduction of the impacts transmitted to the reduction drive of the actuator a single DOF prototype was developed and impact tests were performed. Results demonstrate that the effect of both elasticities (transmission and soft cover) is significant and their combination can further enhance the protection of the drive when compared to the effect of the transmission elasticity or the soft cover alone. As future development we consider to investigate also how to integrate the control in order to tune the active impedance of the system and minimize the effect of the impacts on the robot drive.

The paper is structured as follows. Section II presents the specifications, the functional principle and the design of the high performance modular joint. Section III introduces the simulated model of the experimental set-up while Section IV discusses the test method and the experimental results from the impact trials. Finally, the work concludes in Section V.

II. Development of an High Performance Joint

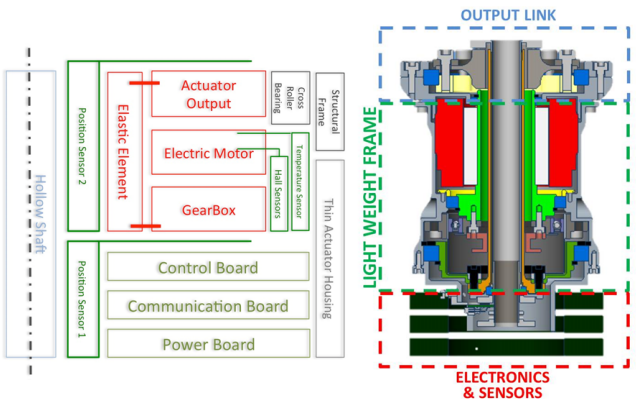

Fig. 3: Schematic of the WALK-MAN actuation unit layout and CAD section. The picture on the left highlights the main functional components and their functional interconnection; while on the right an example of implementation of the logical layout in the real prototype is shown.

The main objective of the development of this novel actuation drive is to realize a modular unit which can be used to power a full-scale humanoid platform, taking care and focusing on some of the main deficiencies (in terms of power density, peak power and physical robustness) of existing motorized actuation technologies. Moreover in the engineering side of this actuation unit others aspects were taken in great consideration including modularity, scalability and reliability, all functional key factors for the design layout towards an actuator that can satisfy the requirements of a humanoid robot, not only in terms of torque, speed and stiffness, but also in terms of uniformity of interfaces (modularity), costs and maintenance.

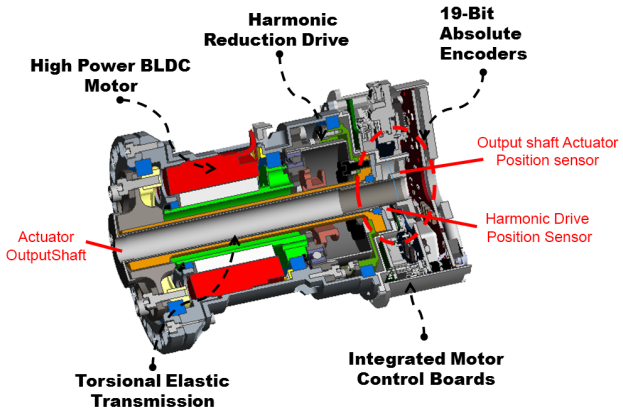

Fig. 4: 3D section of the high power actuator unit (A). Picture shows the assembly of the main components of the actuation unit.

The proposed actuation family consist of (as shown in Fig. 2) three actuation units with three different classes with a continues power (900, 500 and 222 W), size of (D:110 x L:150, D:100 x L:140 and D:60 x L:100 mm) and weight of (2, 1.5 and 0.7 kg) together with the capability to easy change and adapt (during the assembly phases) the reduction ratio and the stiffness to the requirements of each joint of the robot (Tab:I). Each actuation unit is a Series Elastic Actuator (SEA), equipped with embedded driver electronics and a variety of sensing that provides monitoring of the full state of the actuator including position, torque and temperature permitting the implementation of multiple control strategies. Figs. 3-4 shows the cross section of the assembly of the high power actuation unit (A, in Tab.I) demonstrating the interconnection of the main components.

A. Mechanical Design

The actuator unit consists of a frameless brushless DC motor, an Harmonic Drive (HD) gearbox [21], with reduction ratios comprised between 50:1 and 150:1 (G in Tab.I), and a flexible element (a torsion bar) that connect the output of the gearbox to the output flange of the actuator, Fig. 4. The assembly of the motor, HD and the torsion bar, as well as the actuator housing was fully customized to reduce size and weight. In detail, the motor rotor has been designed to minimize its inertia and allow the realization of a hollow through design. These kinds of customizations resulted in actuator with a through-hollow shaft, along the whole length of the actuator. This permitted to place and pass the torsional bar through the center of the actuator. The stator is made with a special winding insulation with high-temperature superior electrical properties that provides an improved breakdown strength and the capacity to work at high temperatures (up to 220°C). The Harmonic Drive gears have been selected from the CPL series (size 25 and 20) for the big and medium size respectively and CSD series (size 17) for the smaller one, both optimized for lightweight applications, moreover these series are characterized by the presence of a central hole, that is large enough to allow the central placement of the torsional bar. The actuator was designed to be lightweight, for this reason its external frame is not structural, except the output link to link interconnection flanges where the cross-roller bearing is placed. Each actuator unit can be mounted on the frame of the robot with a single support connection preventing the loads to be transmitted to the rest of the actuator body apart from the link to link interconnection flanges, Fig.3.

For the implementation of the elastic element the torsion bar concept has been chosen for its linearity and low hysteresis properties when the deflection is inside the elastic region. Fig.5 introduces experimental torque to deflection profiles for different bar stiffness levels. The key parameters for the design of the torsion bar are the material Young modulus, length and external/internal diameters of the bar. Moreover for an actuator that aims to be modular to be implemented in different robot design, it is an essential feature to have the ability to easily vary the stiffness of the bar without major design and fabrication changes. This eventually allow to select and tune the stiffness of the joint without radically redesign. Fig.6 presents the repeatability and the error of the real bar stiffness with respect to the designed stiffness for a number of fabricated torsional bars with design stiffness in the level of 500, 1000, 2200, 2500, 7000, 8000 and 10000Nm/rad due to the manufacturing tolerances and the dispersion due to the variability of the

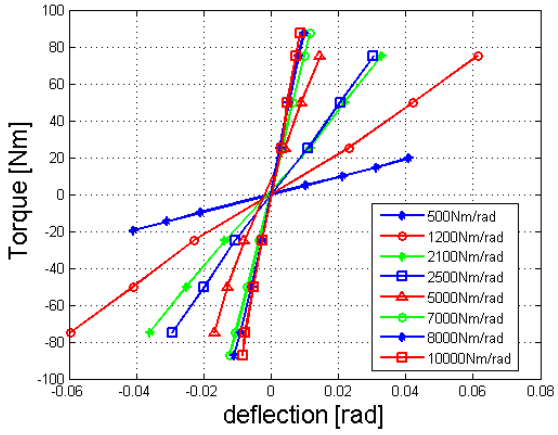

Fig. 5: Experimental Torque vs. Deflection for different torsion bar stiffness.

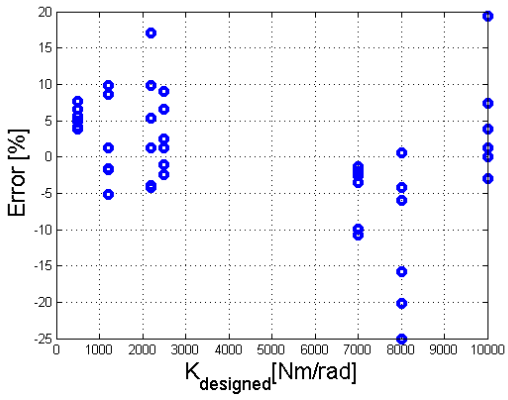

Fig. 6: Error distribution of the measured stiffness w.r.t. the designed stiffness, due to the manufacturing and material tolerances.

materials properties. Errors are evaluated as the difference of designed bar stiffness and the stiffness trend line from experimental data (Fig.5).

The actuator unit is equipped with a complete set of sensors for measuring the joint position, torque and temperature. As shown in Fig.3 linear Hall sensors are adopted for the commutation of the motor phases to implement a full field oriented control of the motor current. Two absolute high resolution position sensors (IC-Haus/Balluff 19-bit) are employed to read the output of the actuator unit, the first is mounted at the output of the harmonic drive and before the torsional bar while the second at the link side after the torsional bar. Such kind of arrangement allows to realize a torque sensor embedded in the mechanical design of the actuator by simply reading the relative deflection of the torsion bar with the two absolute encoders when the unit exerts a certain torque. One of the advantages of this torque measurement principle is that the torque sensor is based on the measurements of the two encoders rather than on Strain Gauges providing a signal with lower noise and it is relatively low cost, both in term of money and mechanical size. In the realization of the torque sensor unit the intrinsic stiffness of the torsion bar plays an important role, and its selection is a compromise between an acceptable resolution of the sensor and a good behavior for resilience and actuator controllability. In the first joint prototype the desired torque resolution for the given encoder resolution was used to set the bar stiffness. Regarding the minimum resolution that allows controlling the system we considered the detent torque of the motor after gearbox. It is a good practice to have a torque measurement resolution at least 10 times bigger than the expected value of the detent torque, consequently, the resultant maximum stiffness value that ensure this is approximately $10000Nm/rad$. A good compromise between resolution and resilience/filtering of impact forces based on simulations was chosen to be $K_s = 2300Nm/rad$ which gives a torque measurement resolution of $57mNm$. Finally, two temperature sensors are integrated in the actuator, the first monitor the motor winding temperature while the second is embedded in the power MOSFETs.

B. Motor Driver Electronic Design

The motor driver and communication electronics have been designed to be fully integrated in the motor assembly (as shown in Fig.s 2(a) and 2(b)). The electronics consists of a stack of three layers with board to board connections that eliminates the wiring. Each layer incorporate different functions: the bottom one accommodates the logic circuits and the communication interface, the second is the power management board, while the third is the power inverter. Only three wires are required to connect an actuator into a kinematic chain: power, ground and communication cable. EtherCAT technology offers hard real time communication and allows to make a daisy-chain network reducing and simplifying the robot wiring. Connectors' location on the boards guarantees easy access to data and power signals.

III. Simulations

We derived a non-linear 1DoF model to investigate the behavior of the actuator when an impact occurs. A detailed description of the experimental setup is reported in Sec. IV. A logical scheme of the model is reported in Fig.7 and the dynamics is described by (1)

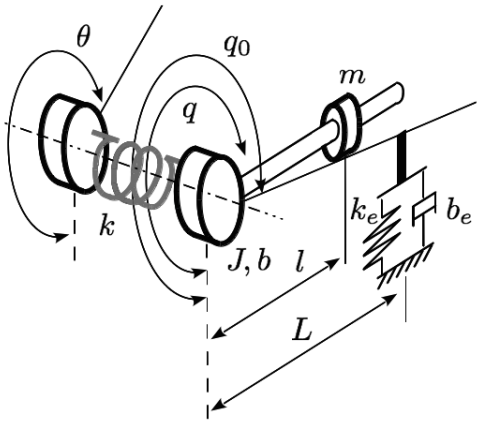

Fig. 7: Schematic of the dynamic model of the experimental set-up realized for testing the actuator. Numerical data used for the simulations are: $J = 0.43kgm^2$, $k = 2300Nm/rad$, $b = 0.5Nms/rad$, $m = 4.2kg$, $g = 9.81$, $l = 0.32$, $L = l$, $k_e = 2000N/m$, $b_e = 50Ns/m$, $q_0 = 4.2rad$.

$$J\ddot{q} + k(q - \theta) + b\dot{q} + mgl\sin(q) = -FL\,, \qquad (1)$$

where J is the rotational link inertia, q is the link position, k represents the stiffness of the elastic transmission between the gearbox and the link, θ is the motor position (at the output of the gearbox), b is the damping coefficient at the link side, m is the link mass, g the gravity acceleration l the distance between the link center of mass and the joint axis, L is the distance between the contact point with the environment and the joint axis, and F the contact force exerted by the environment on the link during the impact. The contact is modeled through a combination of spring and damper (with stiffness k_e and damping coefficient b_e) that can interact with

the link when q overcomes the angle q_0. The contact force is expressed by the following equation:

$$F = \begin{cases} 0, & \text{if } q \leq q_0 \vee k_e L(q - q_0) + b_e L\dot{q} \leq 0 \\ k_e L(q - q_0) + b_e L\dot{q}, & \text{otherwise} \end{cases} . \quad (2)$$

Numerical data used for the simulations are reported in the caption of Fig. 7.

We used this model to evaluate and compare the effect of different transmission stiffness levels. In Fig. 8 the link position obtained from the model is compared with the experimental data for a given stiffness transmission of 2300 Nm/rad and an impact with a rigid environment made by an aluminum part showing a good matching both in the free motion and during the impact phase. In Fig. 9 it can be appreciated that the model is able to evaluate the trend of both the motor torque and the force at the contact point during the impact.

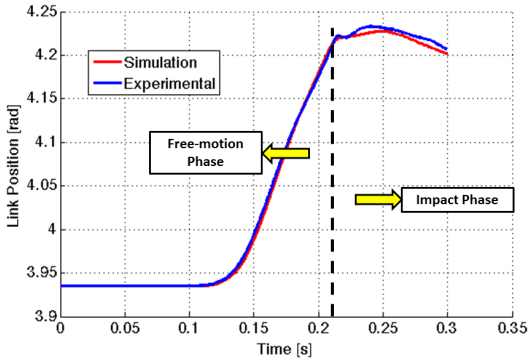

Fig. 8: Comparison between experimental and simulated link position.

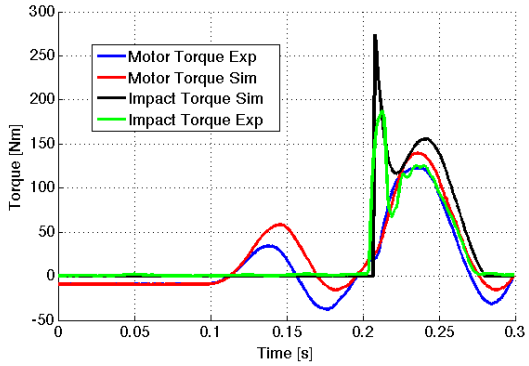

Fig. 9: Comparison between experimental and simulated torque at the motor and the impact torque evaluated as FL.

Once the model has been validated we analyzed the influence of the transmission stiffness on the torque experienced by the gearbox during the impact. The results, summarized in Fig. 10, show that if the stiffness of the torsion bar is lower than a certain value (for the reported case this threshold can be approximately placed at 50000 Nm/rad, a value comparable with the stiffness of the harmonic drives) the peak torque at the motor side is substantially reduced w.r.t. the one given by the peak force at the impact point.

The main drawback of having a low value of the transmission stiffness is the reduction of the actuator bandwidth. In WALK-MAN humanoid the ranges of the transmissions are selected to be in the range where the transmission stiffness reduces significantly the peak torque that can damage the gearbox.

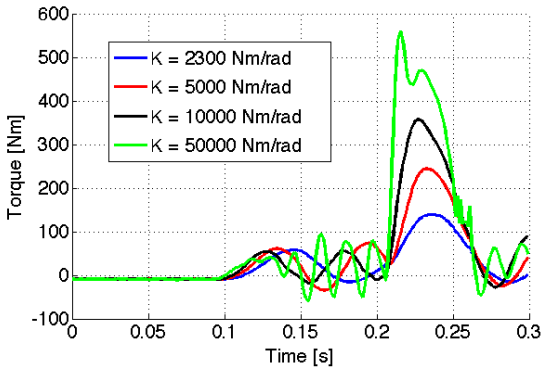

Fig. 10: Motor torque profiles for different transmission stiffness value.

IV. Experimental Tests

Intensive tests were carried out on the actuator to evaluate its performances under severe load condition during impacts. The purpose of these tests is to recreate the load condition on the most stressed joint of a falling robot; changing the ground stiffness is equivalent to investigate how stresses on the joints are modulated by different soft cover padding.

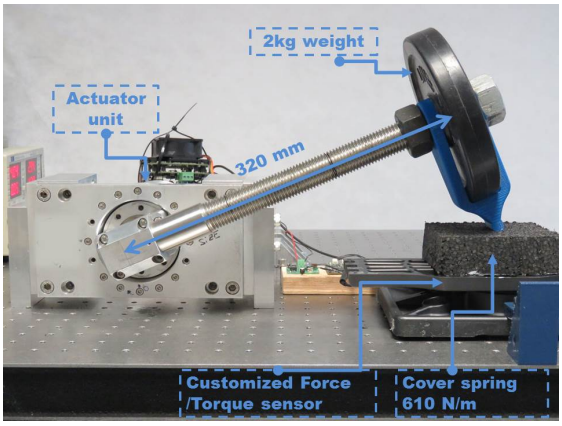

Fig. 11: The Experimental Setup is composed by an actuation unit, a hammer system, a F/T sensor and rigid and soft covers with different stiffness.

As a practical reference of our investigation one of the shoulder joint of the WALK-MAN robot has been taken in consideration. As Fig.1 shows, the robot, during the DRC, fell down, and the shoulder joint was one of the joint which was mostly stressed (the impact occurred at the upper arm close to the elbow) and consequently one with the higher impact forces.

A. Experimental setup

For the experiments a single DOF prototype has been realized, connecting the actuation unit to a link with a length of $320mm$ and weight of $2kg$ at the end to recreate the robot limb mass and inertia during the impact (Fig.11). The contact during the impact happen on the tip of a custom designed hammer, which has a contact area of 300 mm^2. Due to the set-up arrangement the contact with the ground does not happen when the link is horizontal, for this purpose the test table has been instrumented with a 6 axis force torque sensor to monitor the ground reaction forces ($F_{impact} = \|(F_x, F_z)\|$) and thus compare those with the actuator torque measurements. For the soft padding material the expanded polypropylene (EPP) was used. It is an excellent energy absorbing material that withstands multiple impacts without damage. Its light weight and high strength-to-weight ratio make it a good choice for applications such as vehicle crash protection components. It is available in a large range of densities which correspond to different mechanical properties, allowing to tune the protective pad characteristics depending on the requirements [22]. Furthermore it appears to be appropriate for designing/fabrication robot covers as it can be either molded or machined by common CNC which is more suitable for prototyping, without having its properties degraded as happen for most of the polymers. For the impact tests two blocks of 100x100x50mm, of density $35g/l$ and $60g/l$ were used to obtain linear stiffnesses, of $K_1 = 324N/m$ and $K_2 = 608N/m$ respectively for the robot limb/link cover. For the impact on rigid surface an aluminum block of the same dimensions has been manufactured to ensure the contact with the ground happen at the same height/joint angle ensuring the same gravity load during the impact.

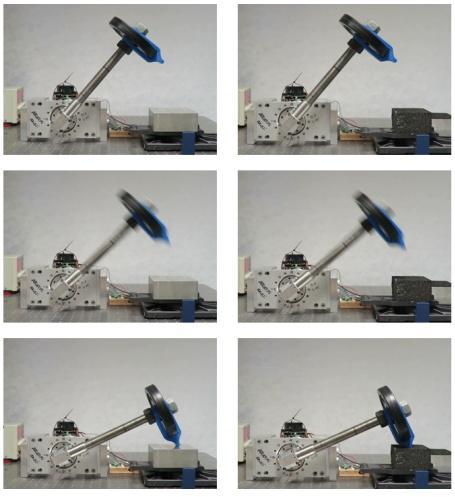

Fig. 12: Photo-sequence of the actuator performing an impact, for both rigid (left) and soft case (right).

The motion controller was implemented on custom DSP-boards. The control loop consists of three nested loops: the inner is a current control loop, executed at $20kHz$, the torque loop is implemented at $5kHz$ and the impedance control is performed at $1kHz$. Actuator and force torque sensor are connected together in a daisy-chain EtherCAT network with an $1kHz$ rate communication with the host PC. To acquire the experimental data a custom user interface has been developed.

B. Results

Experiments can be grouped as follow: Rigid case $K = \infty$, Soft case 2 with $K_2 = 608N/m$ and Soft case 1 with $K_1 = 324N/m$.

The purpose of the $Rigid \;\; case$ experiments is to evaluate the loads on the actuator during impacts with respect to the angular velocity and the controller parameters when the robot has no protective covers. During experiments the torque at the actuator has been kept below 200Nm, impact forces has been controlled modulating the angular velocity and the final position through a ramp trajectory as input, Fig.12 presents the photo-sequence of the impacts for both rigid and soft case.

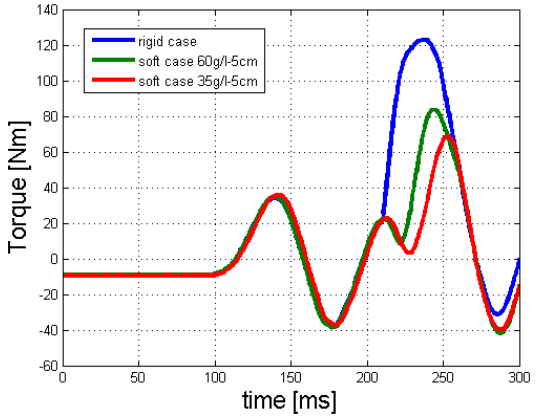

(a)

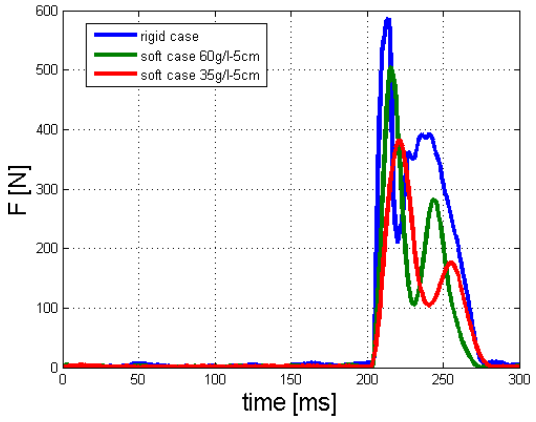

(b)

Fig. 13: Picture show the torque measurements on the joint side a) and force measurements on the F/T sensor side b) for three different level of stiffness (ground side).

Figure13(a) shows the peak torque at the impact while Fig.13(b) shows the ground reaction forces. It is worth noticing that while the contact force have two peaks between 200 and 250 ms due to a bounce of the hammer, the torque

shows only one. On the motor side impact loads are filtered thanks to the dynamics of the compliant system. It is possible to appreciate how reducing the soft cover stiffness the peak amplitude is reduced, in Fig.13(a) motor peak torque vary between 120 and 70 Nm and the impact time is extended, in Fig.13(b) it increase from 11ms to 18ms. Furthermore comparing Fig.13(a) and Fig.13(b) is possible to evaluate the delay of the motor peak torque w.r.t. the peak force due to the impact load travelling time.

V. CONCLUSIONS

In this paper the design and implementation of a novel family of Series Elastic Actuation units was presented. This modular actuation was developed to be the building block of the high performance humanoid WALK-MAN, one of the finalist of the Darpa Robotic Challenge 2015. One of the main features of the presented actuation unit is its robustness and resilience against impacts (e.g. caused by falls). The protection against impacts is achieved with the use of elastic transmission combined with soft cover elements on the link side. After the presentation of the main features of the actuator design and implementation, the effect of the soft cover and series elastic transmission on the reduction of the impact forces during induced impacts have been discussed and demonstrated with simulations and experimental results. The experimental results on the proposed compliant joint design show the combined impact filtering effects of the two elastic components used in the joint (elastic transmission and link cover) and suggest that with appropriate selection and tuning of their elastic properties the protection of the joint against impacts can be maximized. Future work will involve and compare the effects and benefits of the introduction of impedance control and/or the adoption of reaction policies to further reduce or even eliminate the peak load on the motor side.

VI. ACKNOWLEDGMENT

The authors want to thank Lorenzo Baccelliere, Alberto Brando, Stefano Cordasco, Andrea di Basco, Philip Hudson, Alessio Margan, Marco Migliorini, Luca Muratore and Gianluca Pane for their valuable support in the development of the hardware prototypes.

REFERENCES

[1] Ill-Woo Park, Jung-Yup Kim, and Jun-Ho Oh. Online biped walking pattern generation for humanoid robot khr-3(kaist humanoid robot - 3: Hubo). In *Humanoid Robots, 2006 6th IEEE-RAS International Conference on*, pages 398–403, Dec 2006.

[2] Yu Ogura, H. Aikawa, K. Shimomura, H. Kondo, A. Morishima, Hun ok Lim, and A. Takanishi. Development of a new humanoid robot WABIAN-2. In *IEEE International Conference on Robotics and Automation (ICRA 2006)*, pages 76– 81, May 2006.

[3] M. Hirose and K. Ogawa. Honda humanoid robots development. *Philosophical Transactions of the Royal Society of London A: Mathematical, Physical and Engineering Sciences*, 365(1850):11–19, 2007.

[4] S. Lohmeier, T. Buschmann, and H. Ulbrich. System design and control of anthropomorphic walking robot lola. *Mechatronics, IEEE/ASME Transactions on*, 14(6):658–666, Dec 2009.

[5] Y. Ito, S. Nozawa, J. Urata, T. Nakaoka, K. Kobayashi, Y. Nakanishi, K. Okada, and M. Inaba. Development and verification of life-size humanoid with high-output actuation system. In *Robotics and Automation (ICRA), 2014 IEEE International Conference on*, pages 3433–3438, May 2014.

[6] N.G. Tsagarakis, G. Metta, G. Sandini, D. Vernon, R. Beira, F. Becchi, L. Righetti, J. Santos-Victor, A.J. Ijspeert, M.C. Carrozza, et al. icub: the design and realization of an open humanoid platform for cognitive and neuroscience research. *Advanced Robotics*, 21(10):1151–1175, 2007.

[7] Darpa robotics challenge finals 2015.[online]. available:http://www.theroboticschallenge.org/.

[8] NG Tsagarakis, M. Laffranchi, B. Vanderborght, and D.G. Caldwell. A compact soft actuator unit for small scale human friendly robots. In *IEEE International Conference on Robotics and Automation*, pages 4356–4362. IEEE, 2009.

[9] N.G. Tsagarakis, Z. Li, J. Saglia, and D.G. Caldwell. The design of the lower body of the compliant humanoid robot "ccub". In *Robotics and Automation (ICRA), 2011 IEEE International Conference on*, pages 2035–2040. IEEE, 2011.

[10] N.G. Tsagarakis, S. Morfey, G.M. Cerda, Li Zhibin, and D.G. Caldwell. Compliant humanoid coman: Optimal joint stiffness tuning for modal frequency control. In *Robotics and Automation (ICRA), 2013 IEEE International Conference on*, pages 673–678, May 2013.

[11] Sebastian Wolf, Oliver Eiberger, and Gerd Hirzinger. The dlr fsj: Energy based design of a variable stiffness joint. In *Robotics and Automation (ICRA), 2011 IEEE International Conference on*, pages 5082–5089. IEEE, 2011.

[12] M.G. Catalano, G. Grioli, M. Garabini, F. Bonomo, M. Mancinit, N. Tsagarakis, and A. Bicchi. Vsa-cubebot: a modular variable stiffness platform for multiple degrees of freedom robots. In *Robotics and Automation (ICRA), 2011 IEEE International Conference on*, pages 5090–5095. IEEE, 2011.

[13] M. Catalano, G. Grioli, M. Garabini, F.W. Belo, A. di Basco, N. Tsagarakis, and A. Bicchi. A variable damping module for variable impedance actuation. In *Robotics and Automation (ICRA), 2012 IEEE International Conference on*, pages 2666–2672. IEEE, 2012.

[14] Matteo Laffranchi, Nikolaos G Tsagarakis, Ferdinando Cannella, and Darwin G Caldwell. Antagonistic and series elastic actuators: a comparative analysis on the energy consumption. In *Intelligent Robots and Systems, 2009. IROS 2009. IEEE/RSJ International Conference on*, pages 5678–5684. IEEE, 2009.

[15] Amir Jafari, Nikos G Tsagarakis, and Darwin G Caldwell. A novel intrinsically energy efficient actuator with adjustable stiffness (awas). *Mechatronics, IEEE/ASME Transactions on*, 18(1):355–365, 2013.

[16] B. Vanderborght, A. Albu-Schaeffer, A. Bicchi, E. Burdet, D.G. Caldwell, R. Carloni, M. Catalano, O. Eiberger, W. Friedl, G. Ganesh, M. Garabini, M. Grebenstein, G. Grioli, S. Haddadin, H. Hoppner, A. Jafari, M. Laffranchi, D. Lefeber, F. Petit, S. Stramigioli, N. Tsagarakis, M. Van Damme, R. Van Ham, L.C. Visser, and S. Wolf. Variable impedance actuators: A review. *Robotics and Autonomous Systems*, 61(12):1601 – 1614, 2013.

[17] G. Hirzinger, N. Sporer, A. Albu-Schaffer, M. Hahnle, R. Krenn, A. Pascucci, and M. Schedl. Dlr's torque-controlled light weight robot iii-are we reaching the technological limits now? In *Robotics and Automation, 2002. Proceedings. ICRA '02. IEEE International Conference on*, volume 2, pages 1710–1716 vol.2, 2002.

[18] S. Hyon, J.G. Hale, and G. Cheng. Full-body compliant human-humanoid interaction: Balancing in the presence of unknown external forces. *IEEE Transactions on Robotics*, 23(5):884–898, October 2007.

[19] J. Englsberger, A. Werner, C. Ott, B. Henze, M.A. Roa, G. Garofalo, R. Burger, A. Beyer, O. Eiberger, K. Schmid, and A. Albu-Schaffer. Overview of the torque-controlled humanoid robot toro. In *Humanoid Robots (Humanoids), 2014 14th IEEE-RAS International Conference on*, pages 916–923, Nov 2014.

[20] Radford et al. Valkyrie: Nasa's first bipedal humanoid robot. *Journal of Field Robotics*, 32(3):397–419, 2015.

[21] Harmonic drive products homepage.[online]. available:http://harmonicdrive.de/en/home/.

[22] Arpro epp technical documentation.[online]. available:http://www.arpro.com/tech-docs/europe/.